J Ther Eng, Vol. 11, No. 1, pp. 240−253, January, 2025

Journal of Thermal Engineering
Web page info: https://jten.yildiz.edu.tr
DOI: 10.14744/thermal.0000916

Research Article

Impact of memory and long-range interaction in a two-dimensional semi-infinite solid cylinder

Navneet Kumar LAMBA[1,*]

[1]*Department of Mathematics, Shri Lemdeo Patil Mahavidyalaya, Mandhal, 441210, India*

ARTICLE INFO

Article history
Received: 09 December 2023
Revised: 26 February 2024
Accepted: 26 February 2024

Keywords:
Caputo Fractional Derivative; Integral Transformation; Mittag-Leffler Function; Riesz Fractional Derivative; Solid Circular CylinderTemperature; Thermal Stresses; Two Dimensional

ABSTRACT

Space fractional differential operators are used to study long-range interactions, and time differential operators handle memory effects. A semi-infinite circular cylinder is taken into consideration to analyse both effects in a two-dimensional thermoelastic situation where heat conduction is influenced by internal heat generation. A prescribed jump function is applied to the bottom of the semi-infinite circular cylinder, and the time-dependent heat flux happens at the curved edge of the cylinder. The transformative approach of Laplace, Fourier, and Hankel was used to solve the governing equation of heat transfer with Caputo and the finite fractional derivatives of Riesz. The outcomes are expressed in terms of the Bessel function series. The numerical calculations are performed with the material properties of pure copper, and the graphical representations of the thermal distributions are successfully plotted.

Cite this article as: Lamba NK. Impact of memory and long-range interaction in a two-dimensional semi-infinite solid cylinder. J Ther Eng 2025;11(1):240−253.

INTRODUCTION

Many academics and mathematicians have successfully modified numerous previous models of physical phenomena using calculus with fractions during the past few decades. Currently, an exciting and relevant subject in the study of thermoelasticity research is the modelling of the partial differential thermal equation of fractional order (both in time and space). The main advantage of fractional derivatives is that they are capable of evaluating the transfer properties of many types of materials and processes. The general development of fractional derivatives can be found in many books and encyclopaedias by eminent researchers, such as [1−7].

In the study of thermoelasticity of various solids of fractional order, two types of fractional operators are used: time fraction and space fraction. Time fractional operators deal with the memory behaviour, while space fractional operators deal with the interaction over long ranges. A number of studies on memory analysis have been reviewed in recent years by many renowned researchers, such as Povstenko [8-12], Ezzat et al. [13-15], Caputo and Mainardi [16, 17], Said et al. [18], Sherief and Raslan [19, 20], Lamba [21], Lamba and Deshmukh [22, 23], Kumar and Kamdi [24], Verma et al. [25], Youssef [26], and Abouelregal [27]. In order to investigate the mixed bio-convection flow of a nano-fluid containing gyrotactic microorganisms and the mixed convective flow of a micropolar nano-fluid, Rashad

***Corresponding author.**
*E-mail address: navneetkumarlamba@gmail.com

This paper was recommended for publication in revised form by Editor-in-Chief Ahmet Selim Dalkılıç

et al. [28-30] presented the cylinder problem. The effects of chemical reactions on unsteady MHD fluid flow on an infinite vertical plate embedded with porous material and variable suction were numerically investigated by Murali et al. [31, 32].

Compared to temporal modelling, there are only a few studies dealing with long-range interaction due to the complexity of the analytical response of heat with fractional derivatives of Caputo and Riesz. El-Sayed and Gaber [33] explained some important properties of fractional derivatives of Caputo and finite Riesz type and presented the solution of partial diffusion differential equations. The empirical response for the thermoelastic one-dimensional space-time fractional issues was found by Fil'Shtinskii et al. [34] in half-space using the integral transform method. Ciesielski and Leszczynski [35] studied the stationary one-dimensional fractional order numerically based on the finite difference method. Momani [36] solved the spatiotemporal fractional diffusion wave in the context of Caputo sense in a confined spatial domain. Povstenko [37] formulated the thermal stress equations for the generalised Telegraph equation with fractional derivatives of time-spatial order and presented a solution for the nonhomogeneous axisymmetric case. Assiri [38] performed the numerical study considering the one-dimensional time-spatial variable nonlinear fractional thermoelasticity using the finite nonstandard difference approach. The two-dimensional structures space-time fractional heat conduction problem was quantitatively examined by Ozdemir et al. [39] with second order space and time variables in place of anomalous diffusion. In order to investigate the thermal diffusion responses, Atta [40] took into account the Atangana-Baleanu fractional variable problem of an unbounded medium with a spherical cavity.

In the context of a generalised concept of thermoelasticity based on memory dependent components with time delay effects, Abouelregal et al. [41–44] have accomplished some outstanding work. Very recently, Lamba et al. [45] successfully investigated the response of space-time fractional order thermoelastic response in a layer and determined temperature and stress function.

The evolution of memory-containing systems, which are usually complex and dissipative systems, can also be well described by the study of fractional order theory. However, based on the review of the literature, it seems that only one-dimensional heat conduction problems involving fractional space-time derivatives have been studied using numerical methods up to this point. The implications of memory and long-range interaction in two-dimensional thermoelasticity have not been examined till date in the analytical or computational elements of the field. In contrast, the study of different solid bodies based on memory and long-range interactions is very beneficial and urgently required in order to build different material structures, particularly in high-heat engineering applications such as aerospace and space research.

Hence to overcome the gap of research the author motivated to construct a mathematical model by considering a massive circular cylinder of infinite length with a quasi-static approach under both memory and long range interaction effect. To solve the evolved system of fractionally ordered heat equation the integral transform method is used, and the results obtained analytically are measured numerically for a cylinder of pure copper material and presented graphically. Researchers in the material sciences, those developing new materials, and those advancing the theory of thermoelasticity using a quasi-static method utilizing fractional calculus may find great value in this work. Finally, the main objective or aspect of the current effort is to understand how memory and long-range interactions affect the thermal behaviour of a two-dimensional solid with certain boundaries.

MODELING OF THE THERMOELASTIC PROBLEM

To examine the exact thermal behaviour, the spatiotemporal fractional nonhomogeneous boundary region valued problem of heat conduction in a semi-infinite circular cylinder with extension $0 \le r \le b$, $0 \le z < \infty$ is taken into account together with heat generation $g(r,z,t)$. (The physical structure of the potential problem is shown in Fig. 1.) The jump function $P(t)$ is prescribed on the bottom surface ($z = 0$) of a semi-infinite circular cylinder, and a time-dependent heat flux $f(z,t)$ is applied at the curved circular border ($r = b$). The integral transform approach is employed to solve the governing heat transfer, which has Caputo and Riesz's finite fractional derivatives.

This type of modeling by mathematical approach will be beneficial in solving engineering challenges, mostly in

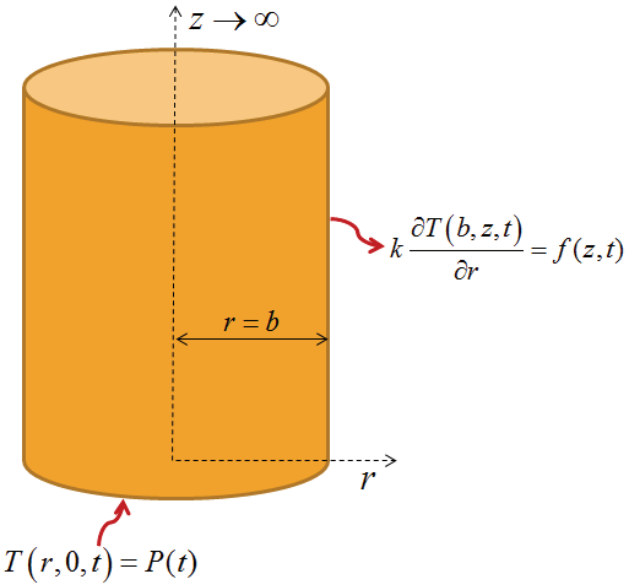

Figure 1. Geometry of a space-time semi-infinite cylinder.

the development of new structural materials. Researchers studying materials, developing new materials, and attempting to improve the theory of thermoelasticity using a quasi-static approach and fractional calculus may also find the outcomes obtained in this article useful.

Space-time Fractional Heat Transfer Equation

The semi-infinite circular cylinder's temperature with space-time fractional-order derivatives satisfying the differential equation,

$$\frac{\partial^2 T}{\partial r^2}+\frac{1}{r}\frac{\partial T}{\partial r}+\frac{\partial^\beta T}{\partial z^\beta}+\frac{g(r,z,t)}{K}=\frac{1}{a}\frac{\partial^\alpha T(r,z,t)}{\partial t^\alpha};\quad 0<\alpha<2,\ 1<\beta<2 \tag{1}$$

Initial and boundary constraints as

$$T(r,z,t)\big|_{z=0}=P(t) \tag{2}$$

$$k\frac{\partial T(r,z,t)}{\partial r}\bigg|_{r=b}=f(z,t) \tag{3}$$

$$T(r,z,t)\big|_{t=0}=0,\ 0<\alpha\le 1, \tag{4}$$

$$\frac{\partial T(r,z,t)}{\partial t}\bigg|_{t=0}=0,\ 1<\alpha<2. \tag{5}$$

Here $T(r,z,t)$ denotes the temperature, K and a are, respectively, the material's thermal conductivity & thermal diffusivity, $P(t)$ denotes the prescribed jump function, $g(r,z,t)/K$ denotes a rate at which heat is produced inside the cylinder and $f(z,t)$ denotes the applied time-dependent heat flux.

In the formation of heat equation (1), both space-time fractional-order derivatives are assumed here $\partial^\alpha / \partial t^\alpha$ stands for Caputo type time fraction derivation of order α and $\partial^\beta / \partial z^\beta$ represent the Riesz space fraction derivation of order β. Many complicated systems, including the multi-scaling of time and spatial variables, exhibit aberrant behaviour that can be explained by this kind of assumed modelling.

Hence, these kinds of thermoelastic problems can be used to study the dynamics of viscoelastic materials like polymers, the atmosphere's pollution diffusion, cell-diffusion processes, signals theory, control theory, electromagnetic theory, etc.

Displacement Potential and Thermal Stresses

The displacement temperature relationship for thin circular cylinders within the framework of two-dimensional thermoelasticity takes the following form [46]:

$$(1-\nu)U_{i,jj}+(1+\nu)e_{,i}=2(1+\nu)a_t T_{,i} \tag{6}$$

$$e=U_{j,j};\quad j,i=1,2 \tag{7}$$

where U denotes the component of displacement, e denotes dilation, ν and a_t, respectively, stands for notation of Poisson's ratio & thermal expansion coefficient of the copper pure material cylinder.

Introducing

$$U_i=\Omega_{,i};\quad i=1,2 \tag{8}$$

One have

$$\nabla^2\Omega=(1+\nu)a_t T$$
$$\sigma_{ik}=2\mu\left(\Omega_{,ik}-\delta_{ik}\Omega_{jj}\right);\ i,j,k=1,2 \tag{9}$$

where δ_{ik} represents the Kronecker delta sign and μ is the Lame constant.

For axial symmetry case

$$\Omega=\Omega(r,z,t),\ T=T(r,z,t) \tag{10}$$

The displacement potential function Ω's differential equation is written as

$$\frac{\partial^2\Omega}{\partial r^2}+\frac{1}{r}\frac{\partial\Omega}{\partial r}=(1+\nu)a_t T \tag{11}$$

The stress components σ_{rr} and $\sigma_{\theta\theta}$ are expressed as

$$\sigma_{rr}=-\frac{2\mu}{r}\frac{\partial\Omega}{\partial r} \tag{12}$$

$$\sigma_{\theta\theta}=-\frac{2\mu}{r}\frac{\partial^2\Omega}{\partial r^2} \tag{13}$$

The state of traction free surface $r = b$ can be taken as

$$\sigma_{rr}=\sigma_{\theta\theta}=0 \tag{14}$$

Additionally, inside the circular cylinder, in the planar condition of stress

$$\sigma_{rz}=\sigma_{zz}=\sigma_{\theta z}=0$$

Therefore, for it to assess the displacement and thermal stress expressions in the assumed domain, it is essential to first study the temperature distribution function from equation (1) with conditions (2) to (5).

Equations (1) to (14) show the mathematical modelling of the two-dimensional space-time fraction problem of thermoelasticity under investigation.

Solution of Space-time Fractional Heat Transfer Equation

To simplify the transfer of heat stated in equation (1) with space-time derivatives of fractional order, the first

definition of Caputo fractional derivative of function $T(t)$ is defined as in Povstenko [5]:

$$\frac{d^{\alpha}T(t)}{dt^{\alpha}} = \frac{1}{\Gamma(n-\alpha)}\int_0^t (t-\tau)^{n-\alpha-1}\frac{d^{n}T(\tau)}{d\tau^{n}}\,d\tau,$$
$$\text{for } t>0\ ,\ n-1<\alpha<n,$$

with the rule of Laplace transform as

$$L\left\{\frac{d^{\alpha}T(t)}{dt^{\alpha}}\right\} = s^{\alpha}\,L\{T\} - \sum_{p=0}^{n-1} T^{(p)}(0^{+})\,s^{\alpha-1-p},$$
$$\text{for } n-1<\alpha<n, \tag{15}$$

where, s is the parameter and n is a positive integer and p = 1, 2, 3, ..., n-1.

On applying the transform specified in equation (15) to (1) and using the corresponding initial conditions (4) and (5), one obtains

$$\frac{\partial^2\overline{T}}{\partial r^2} + \frac{1}{r}\frac{\partial\overline{T}}{\partial r} + \frac{\partial^{\beta}\overline{T}}{\partial z^{\beta}} + \frac{\overline{g}(r,z,s)}{K} = \frac{1}{a}s^{\alpha}\overline{T}(r,z,s) \tag{16}$$

In Laplace's domain, the boundary conditions change to

$$\overline{T}(r,z,s)\big|_{z=0} = \overline{P}(s) \tag{17}$$

$$k\frac{\partial\overline{T}(r,z,s)}{\partial r}\bigg|_{r=b} = \overline{f}(z,s) \tag{18}$$

Secondly, for the variable z, we express the finite Fourier integral transform and its inverse formula over the range $0 \le z < \infty$ as

$$\overline{\overline{T}}(r,\zeta,s) = \int_{z=0}^{\infty} K(\zeta,z')\,\overline{T}(r,z',s)\,dz' \tag{19}$$

$$\overline{T}(r,z,s) = \int_0^{\infty} K(\zeta,z)\,\overline{\overline{T}}(r,\zeta,s)\,d\zeta \tag{20}$$

where

$$K(\zeta,z) = \sqrt{\frac{2}{\pi}}\sin(\zeta,z)$$

Equation (1) contains the Riesz space fraction derivation of order β, which is expressed below using [3].

$$\frac{\partial^{\beta}\psi(z)}{\partial z^{\beta}} = \frac{I_{0+}^{2-\beta}\dfrac{d^2\psi(z)}{\partial z^2} + I_{-}^{2-\beta}\dfrac{d^2\psi(z)}{\partial z^2}}{2\cos\dfrac{(2-\beta)\pi}{2}},\ 1<\beta<2, \tag{21}$$

where the fractional integrals of Riemann-Liouville with $(2-\beta) > 0$ are

$$I_{0+}^{2-\beta}\psi(z) = \frac{1}{\Gamma(2-\beta)}\int_0^z (z-\zeta)^{1-\beta}\,\psi(\zeta)\,d\zeta, \tag{22}$$

$$I_{-}^{2-\beta}\psi(z) = \frac{1}{\Gamma(2-\beta)}\int_z^{\infty} (\zeta-z)^{1-\beta}\,\psi(\zeta)\,d\zeta. \tag{23}$$

and the sin-Fourier transform of equations (22) and (23) written as

$$F_s\left[I_{0+}^{2-\beta}\psi\right] = \zeta^{-(2-\beta)}\left\{\sin\frac{(2-\beta)\pi}{2}F_c\psi + \cos\frac{(2-\beta)\pi}{2}F_s\psi\right\} \tag{24}$$

$$F_s\left[I_{-}^{2-\beta}\psi\right] = \zeta^{-(2-\beta)}\left\{-\sin\frac{(2-\beta)\pi}{2}F_c\psi + \cos\frac{(2-\beta)\pi}{2}F_s\psi\right\} \tag{25}$$

On utilizing the standard results and definition stated above (in equations (19) and (21) to (25)) to (16) and using the corresponding conditions (17), one obtains

$$\frac{\partial^2\overline{\overline{T}}}{\partial r^2} + \frac{1}{r}\frac{\partial\overline{\overline{T}}}{\partial r} - \zeta^{\beta}\overline{\overline{T}} + \zeta^{\beta-1}\overline{P}(s) + \frac{\overline{\overline{g}}(r,\zeta,s)}{K} = \frac{1}{a}s^{\alpha}\overline{\overline{T}}(r,\zeta,s) \tag{26}$$

and transformed boundary becomes

$$k\frac{\partial\overline{\overline{T}}(r,\zeta,s)}{\partial r}\bigg|_{r=b} = \overline{\overline{f}}(\zeta,s) \tag{27}$$

Over the variable r in the range $0 \le r \le b$, the Hankel transform and its inverse transform are described as

$$\overline{\overline{T}}(\beta_m,\zeta,s) = \int_{r'=0}^{b} r'\,K_0(\beta_m,r')\,\overline{\overline{T}}(r',\zeta,s)\,dr' \tag{28}$$

$$\overline{\overline{T}}(r,\zeta,s) = \sum_{m=1}^{\infty} K_0(\beta_m,r)\,\overline{\overline{T}}(\beta_m,\zeta,s) \tag{29}$$

where

$$K_0(\beta_m,r) = \frac{\sqrt{2}}{b}\frac{J_0(\beta_m r)}{J_0(\beta_m b)} \tag{30}$$

here β_1, β_2, β_1, ... are the roots of the transcendental equation

$$J_1(\beta_m,b) = 0 \tag{31}$$

The below result is obtained by employing the integral transform stated in equation (28) to the system of equations (26) and (27).

$$\overline{\overline{\overline{T}}}\left(\beta_m,\xi,s\right)=\frac{a\xi^{\beta-1}\overline{P}(s)}{\left[s^{\alpha}+a\left(\beta_m^2+\xi^{\beta}\right)\right]}+\frac{A(\beta_m,\xi,s)}{\left[s^{\alpha}+a\left(\beta_m^2+\xi^{\beta}\right)\right]} \quad (32)$$

where

$$A(\beta_m,\xi,s)=\frac{abK_0\left(\beta_m,b\right)}{k}\overline{\overline{f}}(\xi,s)+\frac{a\,\overline{\overline{\overline{g}}}(\beta_m,\xi,s)}{K}$$

The final expression of temperature is obtained by inverting the Laplace, Fourier, and Hankel transformations. By employing the inversion formula stated in equations (20) and (29) to (32), one obtains

$$T(r,z,t)=\frac{2a}{b\sqrt{\pi}}\int_0^{\infty}\left\{\sum_{m=1}^{\infty}\sin(\xi z)\frac{J_0(\beta_m r)}{J_0(\beta_m b)}\xi^{\beta-1}\left(\int_0^t\tau^{\alpha-1}E_{\alpha,\alpha}\left[-a\left(\beta_m^2+\xi^{\beta}\right)\tau^{\alpha}\right]P(t-\tau)d\tau\right)\right\}d\xi$$
$$+\frac{2}{b\sqrt{\pi}}\int_0^{\infty}\left\{\sum_{m=1}^{\infty}\sin(\xi z)\frac{J_0(\beta_m r)}{J_0(\beta_m b)}\left(\int_0^t\tau^{\alpha-1}E_{\alpha,\alpha}\left[-a\left(\beta_m^2+\xi^{\beta}\right)\tau^{\alpha}\right]A(\beta_m,\xi,t-\tau)d\tau\right)\right\}d\xi \quad (33)$$

where

$$L^{-1}\left\{\frac{1}{\left[s^{\alpha}+a\left(\beta_m^2+\xi^{\beta}\right)\right]}\right\}=t^{\alpha-1}E_{\alpha,\alpha}\left[-a\left(\beta_m^2+\xi^{\beta}\right)t^{\alpha}\right];\ \alpha>0,\ a\left(\beta_m^2+\xi^{\beta}\right)>0$$

$E_{\alpha,\alpha}$ denotes the generalized Mittag-Leffler function.

Determination of Displacement and Thermal Stresses

Equation (33) in formula (11) yields

$$\left(\frac{\partial^2}{\partial r^2}+\frac{1}{r}\frac{\partial}{\partial r}\right)\Omega(r,z,t)=\frac{2a(1+\nu)a_t}{b\sqrt{\pi}}\int_0^{\infty}\left\{\sum_{m=1}^{\infty}\sin(\xi z)\frac{J_0(\beta_m r)}{J_0(\beta_m b)}\xi^{\beta-1}\left(\int_0^t\tau^{\alpha-1}E_{\alpha,\alpha}\left[-a\left(\beta_m^2+\xi^{\beta}\right)\tau^{\alpha}\right]P(t-\tau)d\tau\right)\right\}d\xi$$
$$+\frac{2(1+\nu)a_t}{b\sqrt{\pi}}\int_0^{\infty}\left\{\sum_{m=1}^{\infty}\sin(\xi z)\frac{J_0(\beta_m r)}{J_0(\beta_m b)}\left(\int_0^t\tau^{\alpha-1}E_{\alpha,\alpha}\left[-a\left(\beta_m^2+\xi^{\beta}\right)\tau^{\alpha}\right]A(\beta_m,\xi,t-\tau)d\tau\right)\right\}d\xi \quad (34)$$

Following the standard result

$$\left(\frac{\partial^2}{\partial r^2}+\frac{1}{r}\frac{\partial}{\partial r}\right)J_0\left(\beta_m r\right)=-\beta_m^2J_0\left(\beta_m r\right)$$

By resolving equation (34) as follows, one gets the expression of the displacement potential function

$$\Omega(r,z,t)=\frac{-2a(1+\nu)a_t}{b\sqrt{\pi}}\int_0^{\infty}\left\{\sum_{m=1}^{\infty}\sin(\xi z)\frac{J_0(\beta_m r)}{\beta_m^2J_0(\beta_m b)}\xi^{\beta-1}\left(\int_0^t\tau^{\alpha-1}E_{\alpha,\alpha}\left[-a\left(\beta_m^2+\xi^{\beta}\right)\tau^{\alpha}\right]P(t-\tau)d\tau\right)\right\}d\xi$$
$$-\frac{2(1+\nu)a_t}{b\sqrt{\pi}}\int_0^{\infty}\left\{\sum_{m=1}^{\infty}\sin(\xi z)\frac{J_0(\beta_m r)}{\beta_m^2J_0(\beta_m b)}\left(\int_0^t\tau^{\alpha-1}E_{\alpha,\alpha}\left[-a\left(\beta_m^2+\xi^{\beta}\right)\tau^{\alpha}\right]A(\beta_m,\xi,t-\tau)d\tau\right)\right\}d\xi \quad (35)$$

The radial stress function and the angular stress function are expressed using equation (35) in equations (12) and (13), respectively.

$$\sigma_{rr}=\frac{4\mu a(1+\nu)a_t}{b\sqrt{\pi}}\int_0^{\infty}\left\{\sum_{m=1}^{\infty}\sin(\xi z)\frac{J_1(\beta_m r)}{r\beta_mJ_0(\beta_m b)}\xi^{\beta-1}\left(\int_0^t\tau^{\alpha-1}E_{\alpha,\alpha}\left[-a\left(\beta_m^2+\xi^{\beta}\right)\tau^{\alpha}\right]P(t-\tau)d\tau\right)\right\}d\xi$$
$$+\frac{4\mu(1+\nu)a_t}{b\sqrt{\pi}}\int_0^{\infty}\left\{\sum_{m=1}^{\infty}\sin(\xi z)\frac{J_1(\beta_m r)}{r\beta_mJ_0(\beta_m b)}\left(\int_0^t\tau^{\alpha-1}E_{\alpha,\alpha}\left[-a\left(\beta_m^2+\xi^{\beta}\right)\tau^{\alpha}\right]A(\beta_m,\xi,t-\tau)d\tau\right)\right\}d\xi \quad (36)$$

$$\sigma_{\omega\omega}=\frac{4\mu a(1+\nu)a_t}{b\sqrt{\pi}}\int_0^{\infty}\left\{\sum_{m=1}^{\infty}\frac{\sin(\xi z)}{J_0(\beta_m b)}\left(J_0(\beta_m r)-\frac{1}{\beta_m r}J_1(\beta_m r)\right)\xi^{\beta-1}\left(\int_0^t\tau^{\alpha-1}E_{\alpha,\alpha}\left[-a\left(\beta_m^2+\xi^{\beta}\right)\tau^{\alpha}\right]P(t-\tau)d\tau\right)\right\}d\xi$$
$$+\frac{4\mu(1+\nu)a_t}{b\sqrt{\pi}}\int_0^{\infty}\left\{\sum_{m=1}^{\infty}\frac{\sin(\xi z)}{J_0(\beta_m b)}\left(J_0(\beta_m r)-\frac{1}{\beta_m r}J_1(\beta_m r)\right)\left(\int_0^t\tau^{\alpha-1}E_{\alpha,\alpha}\left[-a\left(\beta_m^2+\xi^{\beta}\right)\tau^{\alpha}\right]A(\beta_m,\xi,t-\tau)d\tau\right)\right\}d\xi \quad (37)$$

Special Case

$$g(r,z,t)=g_{pi.}\delta\left(r-r_1\right)\delta\left(z-z_1\right)\delta\left(t-\tau\right)$$
$$f(z,t)=z^2\times\exp[-\omega t],\ \omega>0$$
$$P(t)=\begin{cases}0, & t\le 0\\ 1, & t>0\end{cases}$$

where $\omega = 10 > 0$, δ represents the Dirac-delta function, and r is the radii expressed in metres.

At time $t \to \tau = 1$, heat is released instantly from the heat source $g(r,z,t)$, a significant Instantaneous point heat source positioned in the centre of a semi-infinite circular cylinder in the radial direction r.

Dimensions

A semi-infinite solid cylinder radius is set at $b = 3m$, and a semi-infinite circular cylinder's central circular paths are taken into account while setting $r_1 = 1.5m$.

Material Properties

A thin circular copper (pure) cylinder has been numerically calculated with the following material characteristics [46]:

$$a=112.34\times10^{-6}\left(m^2s^{-1}\right),\ K=386\left(W/mk\right),\ \rho=8954\left(kg/m^3\right),$$
$$c_p=383\left(J/KgK\right),\ \upsilon=0.35\ \ a_t=16.5\times10^{-6}\left(1/K\right),\ \mu=26.67$$

Numerical Analysis

For the purpose of calculating numerically this problem, the following dimensionless variables are introduced.

$$t'=\left(\frac{a}{L^{\beta}}\right)^{\frac{1}{\alpha}}t,\ r'=\frac{r}{b},\ z'=\frac{z}{L},T'=\frac{T}{T_0},\ \sigma'_{ij}=\frac{\sigma_{ij}}{4\mu a_tT_0}$$

It is far more difficult to solve differential equations of fractional (or non-integer) order accurately, consistently, and efficiently than it is to solve them in the typical integer-order case. Moreover, most computer tools do not provide built-in methods for solving problems of this type. So in this study, we use Mathematica software to perform numerical calculations by applying the proposed special case, setting the dimensions for the thin circular copper (pure) cylinder material characteristics, and creating dimensionless forms for all the variables.

All these numerical investigations were observed for all variables to analyse the effects of space-time breaking in a solid cylinder. These calculations are shown in the corresponding figures. Figures 2–6, respectively, show the computational outcomes for the dimensionless temperature

distribution and the dimensionless radial and angular stress distribution along the time, radius, and thickness directions for different values subjected to applied boundaries and heat generation.

Figures 2(a), 2(b), and 2(c), respectively, represent the memory response of the dimensionless temperature, radial stress, and angular versus time (at fixed $r = 0.5$, $z = 1$) for various values of $\alpha(\beta = 2)$. Initially, the temperature, radial

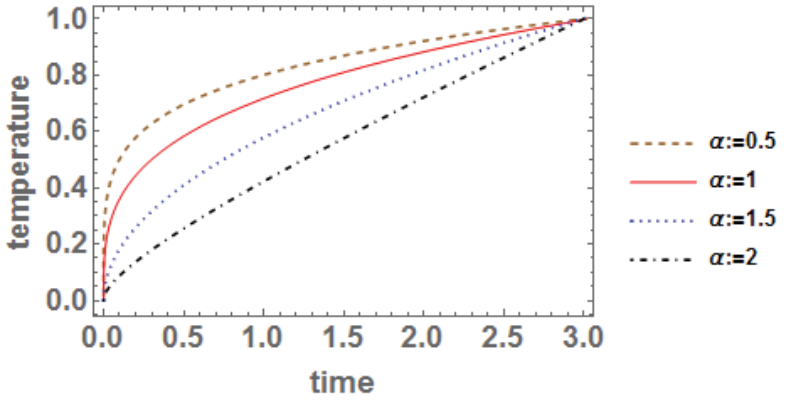

Figure 2. (a) Nondimensional temperature distribution versus time (at $r = 0.5$, $z = 1$) for various values of $\alpha(\beta = 2)$.

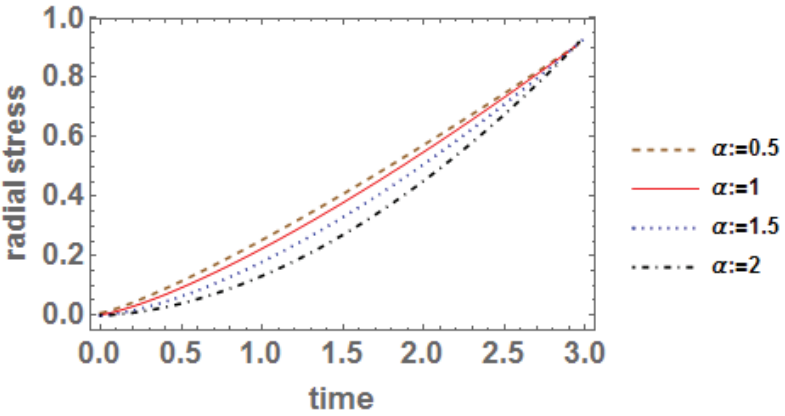

Figure 2. (b) Nondimensional radial stress distribution versus time (at $r = 0.5$, $z = 1$) for various values of $\alpha(\beta = 2)$.

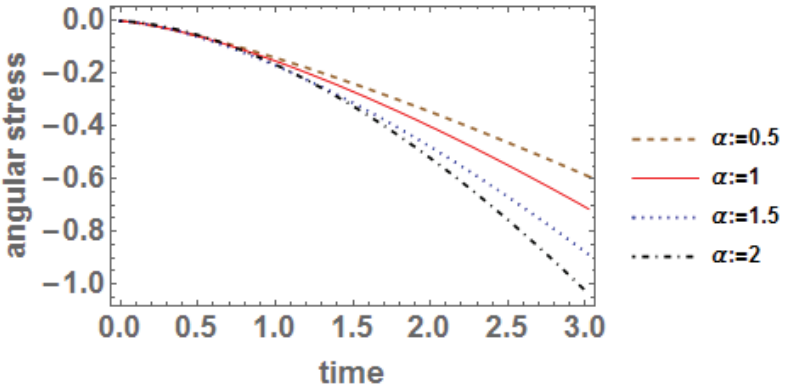

Figure 2. (c) Nondimensional angular stress distribution versus time (at $r = 0.5$, $z = 1$) for various values of $\alpha(\beta = 2)$.

stress, and angular stress functions are zero; further temperature and radial stress increase with time, while vice versa in angular stresses. For the small value of the time fraction parameter, a larger distribution of temperature variation is observed, whereas equilibrium in radial and angular stresses occurs for the small value of the time fraction parameter as compared to the higher values. Also, temperature and stress variations exhibit uniform flow behaviour with respect to time for the fractional-order parameter values of $\alpha = 0.5, 1, 1.5, 2$.

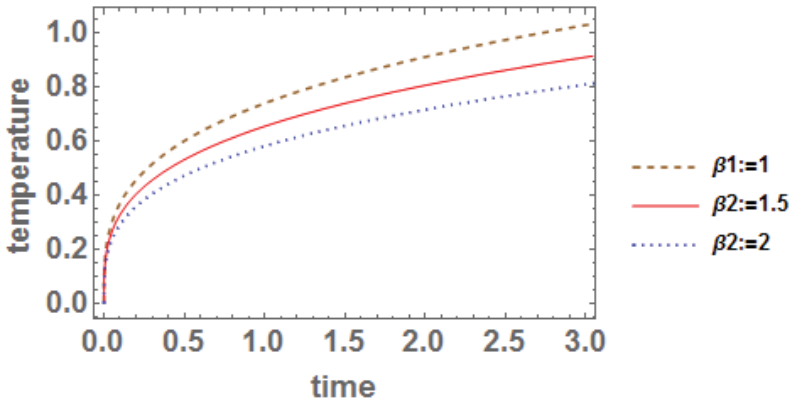

Figure 3. (a) Dimensionless temperature flow versus time (at $r = 0.5$, $z = 1$) for various values of $\beta(\alpha = 1)$.

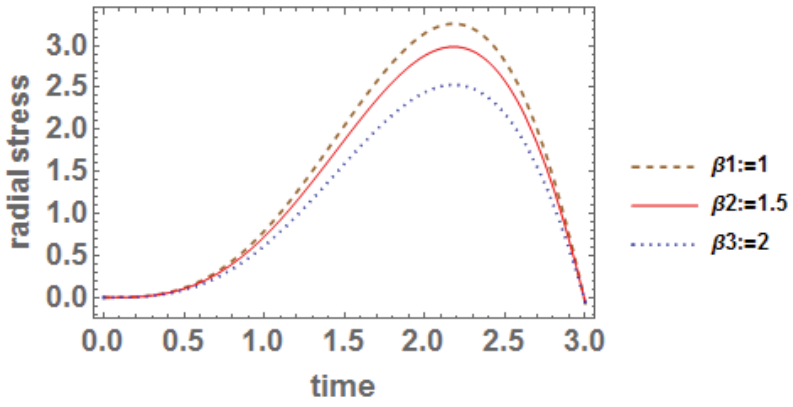

Figure 3. (b) Dimensionless radial stress distribution versus time (at $r = 0.5$, $z = 1$) for various values of $\beta(\alpha = 1)$.

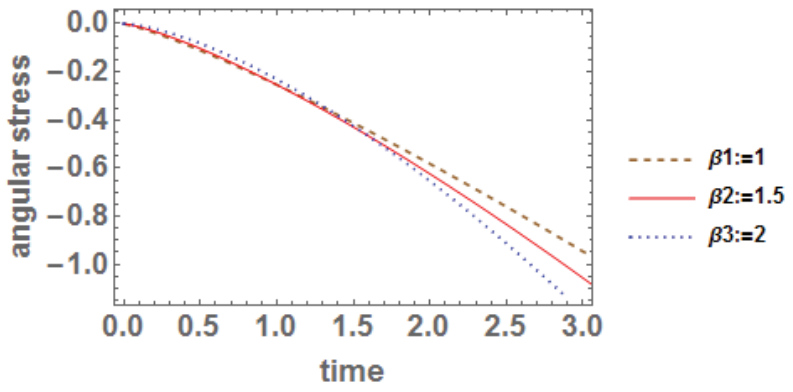

Figure 3. (c) Nondimensional angular stress distribution versus time (at $r = 0.5$, $z = 1$) for various values of $\beta(\alpha = 1)$.

Figures 3(a), 3(b), and 3(c), respectively, represent the long-range interaction impact on non-dimensional temperature, radial stress, and angular versus time (at fixed r = 0.5, z = 1) for various values of $\beta(\alpha = 1)$. At t = 0 temperature, radial stress and angular stress functions are zero; further temperature increases with passage of time, whereas angular stress decreases with increase in time. Radial stress function increases with time, reaches its peak at t = 2, and afterwards is found to be decreasing. The larger distribution in temperature and stresses is observed for a small value of the space-fraction parameter β. Significant discrimination in temperature and stress variations occurs only for high values of time and spatial variables. Hence, it can be concluded that the temperature flow and stress dispersion not

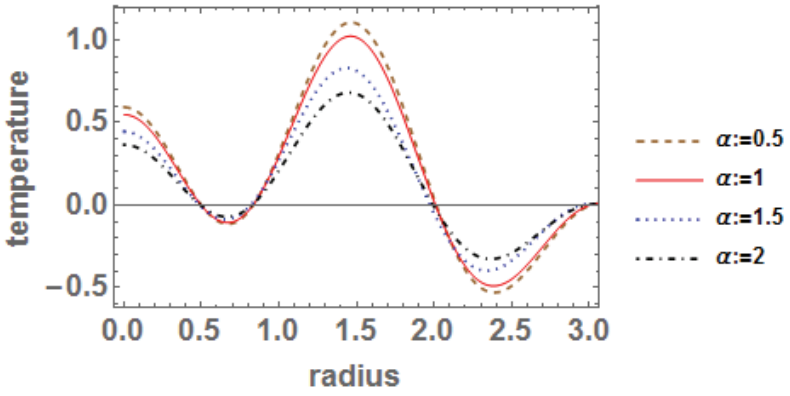

Figure 4. (a) Nondimensional temperature distribution versus radius (at t = 1, z = 1) for various values of $\alpha(\beta = 2)$.

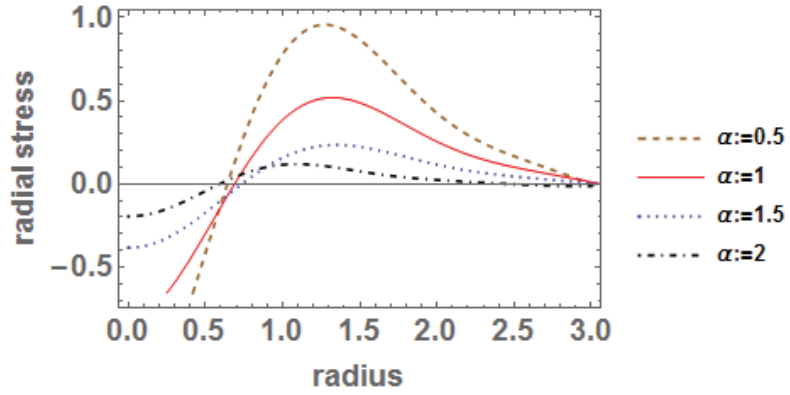

Figure 4. (b) Nondimensional radial stress distribution versus radius (at t = 1, z = 1) for various values of $\alpha(\beta = 2)$.

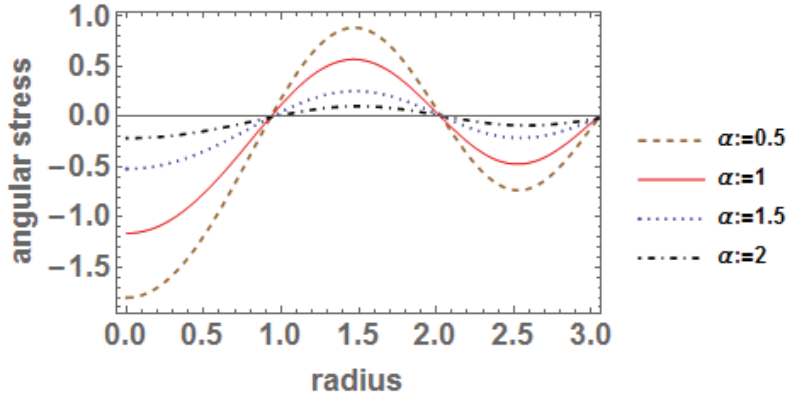

Figure 4. (c) Nondimensional angular stress distribution versus radius (at t = 1, z = 1) for various values of $\alpha(\beta = 2)$.

only depend on the neighborhood values of a selected point but also depend on remote points.

Figures 4(a), 4(b), and 4(c), respectively, show the memory response of the non-dimensional temperature, radial stress, and angular stress versus radius (at fixed $t = 1$, $z = 1$) for various values of $\alpha(\beta = 2)$. From all the plotting, it is found that the maximum distribution of temperature and stresses is observed in the midpoint of the solid cylinder due to the strength of the instantaneous point heat source at $r = 1.5$, and on the outer radii $r = 3$, the variation in temperature and stresses is zero. Also, temperature and stress variations exhibit non-uniform flow behaviour with respect to radius for weak, normal, and superconductivity. Further elevation in distribution occurs for small fractional parameter values;

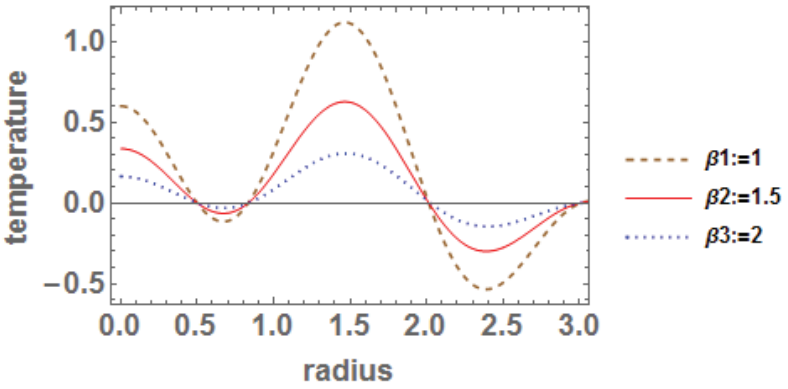

Figure 5. (a) Nondimensional temperature distribution versus radius (at $t = 1$, $z = 1$) for various values of $\beta(\alpha = 1)$.

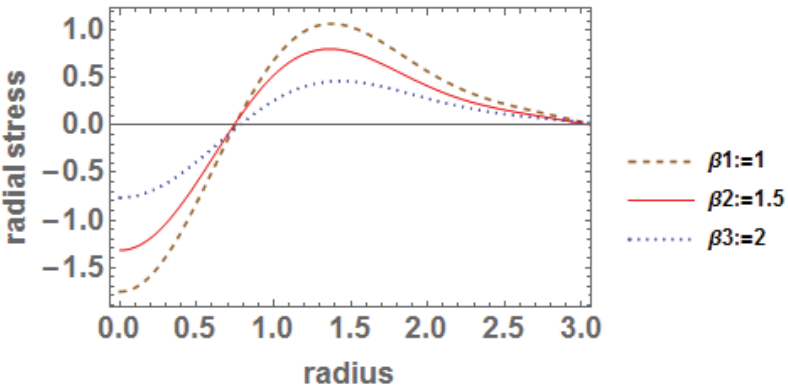

Figure 5. (b) Nondimensional radial stress distribution versus radius (at $t = 1$, $z = 1$) for various values of $\beta(\alpha = 1)$.

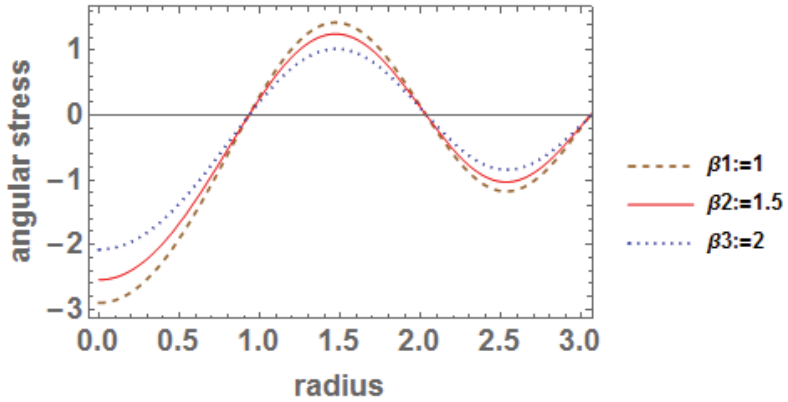

Figure 5. c) Nondimensional angular stress distribution versus radius (at $t = 1$, $z = 1$) for various values of $\beta(\alpha = 1)$.

hence, a significant impact of time-fractional is noted along the radial direction for thermal variation.

Figures 5(a), 5(b), and 5(c), respectively, show the long-range interaction impact on the non-dimensional temperature, radial stress, and angular stress versus radius (at fixed $t = 1$, $z = 1$) for various values of $\beta(\alpha = 1)$. From all the plotting, it is cleared that the maximum distribution of temperature and stresses is observed in the middle of the solid cylinder due to the strength of the instantaneous point heat source at $r = 1.5$, and on the outer radii $r = 3$, variation in temperature and stresses is zero. Further, a significant impact of space-fractional parameters is obtained

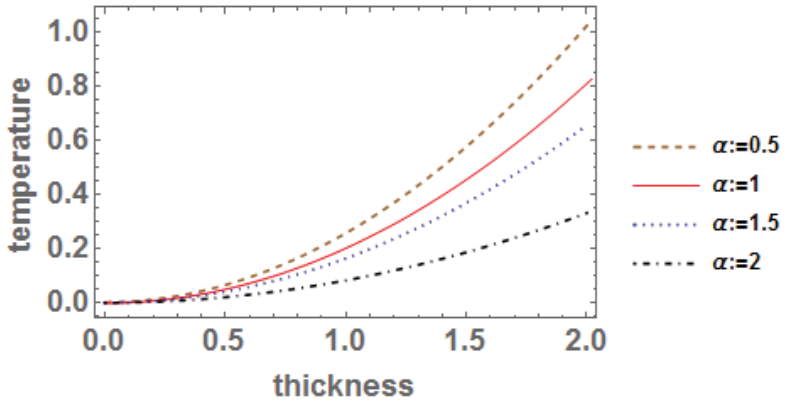

Figure 6. (a) Nondimensional temperature distribution versus thickness (at $t = 1$, $r = 0.5$) for various values $\alpha(\beta = 2)$.

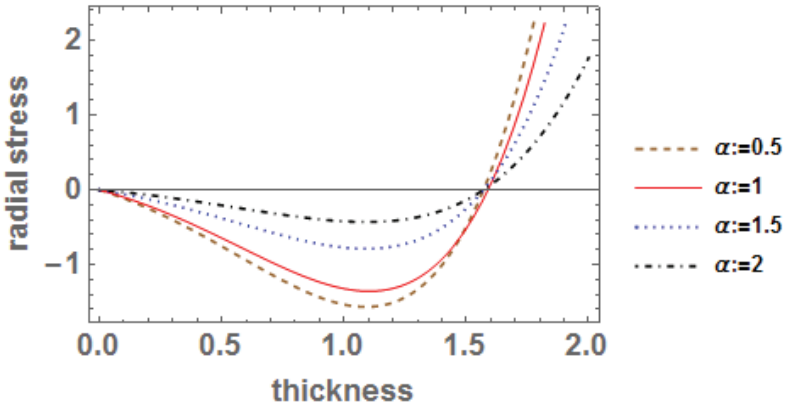

Figure 6. (b) Nondimensional radial stress distribution versus thickness (at $t = 1$, $r = 0.5$) for various values $\alpha(\beta = 2)$.

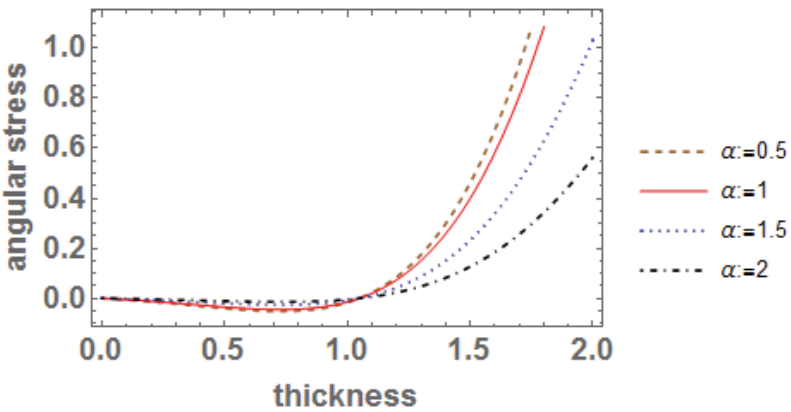

Figure 6. (c) Nondimensional angular stress distribution versus thickness (at $t = 1$, $r = 0.5$) for various values of $\alpha(\beta = 2)$.

from plotting of temperature and stress functions radially. A sufficient discrimination in thermal curve variation is observed for different values of β in temperature and radial stress variation. Radial and angular stresses increase gradually with an increase in radius, reaching their peak at the midpoint and becoming zero at the outer radii. The resultant curve variation is found to be smoother for the greater space-fractional fractional parameter.

Figures 6(a), 6(b), and 6(c), respectively, show the memory impact on the non-dimensional temperature, radial stress, and angular stress versus thickness (at fixed t = 1, z = 1) for various values of $\beta(\alpha = 1)$. Variation in temperature

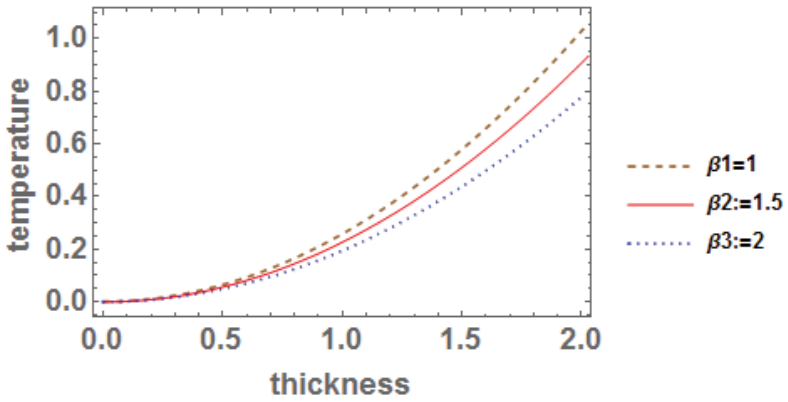

Figure 7. (a) Nondimensional temperature distribution versus thickness (at t = 1, r = 0.5) for various values of $\beta(\alpha = 1)$.

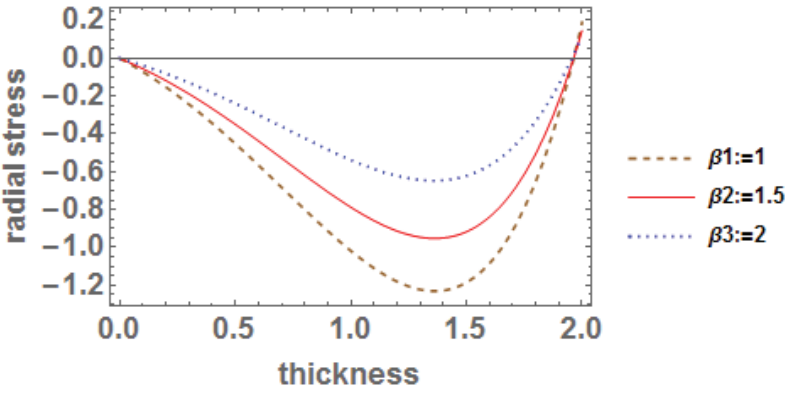

Figure 7. (b) Nondimensional radial stress distribution versus thickness (at t = 1, r = 0.5) for various values of $\beta(\alpha = 1)$.

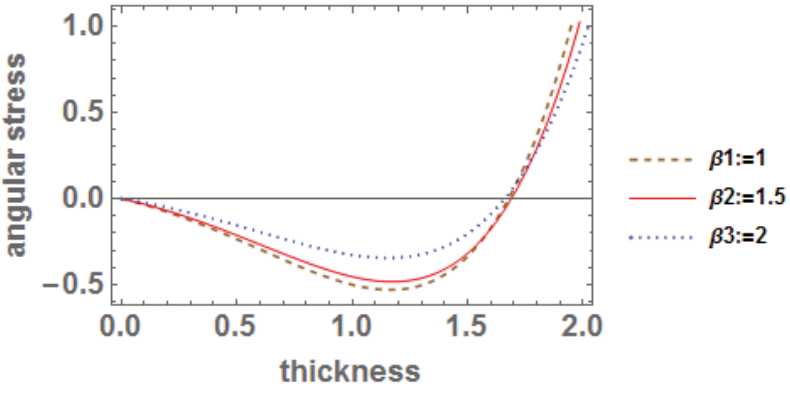

Figure 7. (c) Nondimensional radial stress distribution versus thickness (at t = 1, r = 0.5) for various values of $\beta(\alpha = 1)$.

and thermal stresses increases slowly on moving from lower to upper surfaces, and sufficient discrimination in the plotting of curves is noted for large thicknesses. Hence, it can be concluded that a memory response is sufficiently affected by a large thickness for different time-fractional parameters.

Figures 7(a), 7(b), and 7(c), respectively, represent the long-range interaction impact on the non-dimensional temperature, radial stress, and angular stress versus thickness (at fixed $t = 1$, $z = 1$) for various values of $\beta(\alpha = 1)$. Temperature increases rapidly with thickness for different space fractions, whereas radial stress and angular stress decrease initially with an increase in thickness until $z = 1.25$ and then increase towards the upper plane surface. A sufficient impact of space fractional values is observed for all the plots moving from the lower to the upper face of the cylindrical region. Also, a longer interaction in radial stresses is obtained as compared to angular stress distribution along thickness direction.

The global tendency is predicted by the fractional-order derivative heat equation for space and time. The classical equation of heat conduction for the fractional value of space-time fractional derivatives is interpolated using both the wave equation and the local diffusion equation. Furthermore, as a result of the fractional order theory, the non-local operator anticipates a delayed reaction to natural physical stimuli, in contrast to the instantaneous response to the non-localized generalised theory of heat conduction. In order to better simulate real-world thermoelastic behaviour in the model, space-time fractional-order derivatives studies for various solids are useful in capturing the true behaviours of materials.

The Series Solution Converges

Let's examine at the manner in which the series solution converges.

$$A_m = \left\{ \sum_{m=1}^{\infty} \sin(\zeta z) \frac{J_0(\beta_m r)}{J_0(\beta_m b)} \xi^{\beta-1} \left(\int_0^t \tau^{\alpha-1} E_{\alpha,\alpha} \left[-a\left(\beta_m^2 + \xi^{\beta}\right)\tau^{\alpha} \right] P(t-\tau)\, d\tau \right) \right\}$$

$$B_m = \left\{ \sum_{m=1}^{\infty} \sin(\zeta z) \frac{J_0(\beta_m r)}{J_0(\beta_m b)} \left(\int_0^t \tau^{\alpha-1} E_{\alpha,\alpha} \left[-a\left(\beta_m^2 + \xi^{\beta}\right)\tau^{\alpha} \right] A(\beta_m, \xi, t-\tau)\, d\tau \right) \right\}$$

Then

$$T(r,z,t) = \frac{2}{b\sqrt{\pi}} \left[a \int_0^{\infty} A_m \, d\zeta + \int_0^{\infty} B_m \, d\zeta \right]$$

We have

$$\lim_{m\to\infty} \left| \frac{A_{m+1}}{A_m} \right| < 1, \ \lim_{m\to\infty} \left| \frac{B_{m+1}}{B_m} \right| < 1$$

This implies T converges for all $r > 0$.

RESULTS AND DISCUSSION

In this manuscript, a two-dimensional quasi-static thermoelastic problem of a time-spatially fractional semi-infinite solid circular cylinder with derivatives Caputo's and Riesz fractional order is mathematically modelled. The solution of the governing heat transfer with an internal heat source is studied using the transformative approaches of Laplace, Fourier and Hankel and satisfies the corresponding applied bounds. The thermal behaviour modelled successfully illustrates the memory and remote interaction in the temperature distribution, radial and angular stress for different space-time fraction parameters along the time, radius and thickness directions. Boundary cases of the work, such as the wave equation, Laplace's equation, and diffusion equation, can also be studied and verified using numerical representations.

CONCLUSION

The main observations of the work are discussed down:

1. By fixing $\beta = 2$ and $\alpha = 0$ equation (1), describe the Laplace equation, and its solution and thermal fluctuation within predetermined boundaries can be easily examined from the analytical part above.
2. For $\beta = 2$ and $\alpha = 1$ equation (1) reduces to the classical diffusion equation, and for $\beta = 2$ and $\alpha = 2$ equation (1) describes a wave equation. In both the equations, variation of temperature, radial stress, and angular stress are successfully investigated and examined in the above numerical computation with respect to time, radius, and thickness direction.
3. For $0 < \alpha < 1$; $1 < \alpha < 2$ and $\beta = 2$ equation (1) gives the diffusion equation based on time-fractional, and the impact of memory can be easily seen in temperature and stress distributions, as discussed in graphical plotting.
4. For $1 < \beta < 2$; and $\alpha = 1$ (1) gives the diffusion equation based on space-fractional, and the effect of long-range interaction in temperature and stress distributions is successfully described in numerical computation.
5. For $\alpha = 1, \beta = 1$ and $\alpha = 1, \beta = 1.5$ equation (1) represents the interpolation behaviour for temperature and stress functions.
6. For $1 < \alpha < 2$; $1 < \beta < 2$ equation (1) shows the diffusion equation based on both space-time fractional, and in this range both memory and long-range interaction impact are successfully studied for a two dimensional circular solid with heat generation.
7. A significant impact of temperature, radial and angular stress distribution is noted for different space-time fractional parameters on varying time, radius, and thickness. Hence, it can be concluded that both space and time fractional order parameters may contribute to an important factor in the classification of material properties and be useful in physical processing.
8. The response obtained in this study predicts desired delayed responses to physical stimuli found in nature.

In this study, we have determined both delayed and long-range interactions in a solid circular cylinder for weak, intermediate, and superconductivity. Thermal effects are

also investigated and successfully presented for the two-dimensional problem with semi-infinite length. The results of the study may be useful for the structural design of various objects used in the physical processing of many engineering applications.

NOMENCLATURE

$T(r,z,t)$	Temperature,
K	Material's thermal conductivity
a	Thermal diffusivity
$P(t)$	Jump function
$g(r,z,t)/K$	Rate at which heat is produced inside the cylinder
$f(z,t)$	Time-dependent heat flux
$\partial^{\alpha} / \partial t^{\alpha}$	Caputo type time fraction derivation of order α
$\partial^{\beta} / \partial z^{\beta}$	Riesz space fraction derivation of order β
U	Component of displacement
e	Dilation
ν	Poisson's ratio
a_t	Thermal expansion coefficient
δ_{ik}	Kronecker delta
μ	Lame constant
Ω	Displacement potential function
σ_{rr}	Radial stress
$\sigma_{\theta\theta}$	Angular stress
$E_{\alpha,\alpha}$	Mittag-Leffler function

ACKNOWLEDGEMENT

The Author expresses gratitude to Prof. Dr. Ahmet Selim Dalkılıç, the Editor-in-Chief of the Journal of Thermal Engineering, and all the respected reviewers for their valuable comments for general alterations and improvements intended to enhance the research work.

AUTHORSHIP CONTRIBUTIONS

Authors equally contributed to this work.

DATA AVAILABILITY STATEMENT

The authors confirm that the data that supports the findings of this study are available within the article. Raw data that support the finding of this study are available from the corresponding author, upon reasonable request.

CONFLICT OF INTEREST

The authors declared no potential conflicts of interest with respect to the research, authorship, and/or publication of this article.

ETHICS

There are no ethical issues with the publication of this manuscript.

REFERENCES

[1] Oldham KB, Spanier J. The Fractional Calculus. New York: Academic Press; 1974.

[2] Miller KS, Ross B. An Introduction to the Fractional Calculus and Fractional Differential Equations. New York: Wiley; 1993.

[3] Samko SG, Kilbas AA, Marichev OI. Fractional Integrals and Derivatives Theory and Applications. Amsterdam: Gordon and Breach; 1993.

[4] Podlubny I. Fractional Differential Equations. San Diego: Academic Press; 1999.

[5] Povstenko Y. Fractional Thermoelasticity. In: Hetnarski RB, editor. Encyclopedia of Thermal Stresses. Dordrecht: Springer; 2014. [CrossRef]

[6] Kilbas AA, Srivastava HM, Trujillo JJ. Theory and Applications of Fractional Differential Equations. Amsterdam: Elsevier; 2006.

[7] Diethelm K. The Analysis of Fractional Differential Equations. Berlin: Springer; 2010. [CrossRef]

[8] Povstenko YZ. Two-dimensional axisymmetric stresses exerted by instantaneous pulses and sources of diffusion in an infinite space in a case of time-fractional diffusion equation. Int J Solids Struct 2007;44:2324–2348. [CrossRef]

[9] Povstenko YZ. Theory of thermoelasticity based on the space-time-fractional heat conduction equation. Phys Scr T 2009;136:014017. [CrossRef]

[10] Povstenko YZ. Fractional radial diffusion in a cylinder. J Mol Liq 2008;137:46–50. [CrossRef]

[11] Povstenko YZ. Non-axisymmetric solutions to time-fractional diffusion-wave equation in an infinite cylinder. Frac Calc Appl Anal 2011;14:418–435. [CrossRef]

[12] Povstenko YZ. Time-fractional radial heat conduction in a cylinder and associated thermal stresses. Arch Appl Mech 2012;82:345–362. [CrossRef]

[13] Ezzat MA, EL-Karamany AS, EL-Bary AA. On thermo-viscoelasticity with variable thermal conductivity and fractional-order heat transfer. Int J Thermophys 2015;36:1684–1697. [CrossRef]

[14] Ezzat MA, EL-Karamany AS, EL-Bary AA. Thermo-viscoelastic materials with fractional relaxation operators. Appl Math Modell 2015;39:7499–7512. [CrossRef]

[15] Ezzat MA, EL-Bary AA. Unified fractional derivative models of magneto-thermo-viscoelasticity theory. Arch Mech 2016;68:285–308.

[16] Caputo M, Mainardi F. A new dissipation model based on memory mechanism. Pure Appl Geophys 1971;91:134–147. [CrossRef]

[17] Caputo M, Mainardi F. Linear model of dissipation in elastic solids. Rivista Nuovo Cimento 1971;1:161–1981. [CrossRef]

[18] Said SM, Abd-Elaziz EM, Othman MIA. A two-temperature model and fractional order derivative in a

rotating thick hollow cylinder with the magnetic field. Indian J Phys 2009;97:3057−3064. [CrossRef]
[19] Sherief HH, Raslan WE. A problem in fractional order thermoelasticity theory for an infinitely long cylinder composed of 3 layers of different materials. J Therm Stress 2022;45:234−244. [CrossRef]
[20] Sherief HH, Raslan WE. Fundamental solution for a line source of heat in the fractional order theory of thermoelasticity using the new Caputo definition. J Therm Stress 2019;42:18−28. [CrossRef]
[21] Lamba NK. Thermosensitive response of a functionally graded cylinder with fractional order derivative. Int J Appl Mech Eng 2022;27:107−124. [CrossRef]
[22] Lamba NK, Deshmukh KC. Hygrothermoelastic response of a finite solid circular cylinder. Multidiscip Model Mater Struct 2020;16:37−52. [CrossRef]
[23] Lamba NK, Deshmukh KC. Hygrothermoelastic response of a finite hollow circular cylinder. Waves Random Complex Media 2022;2030501:1−16. [CrossRef]
[24] Kumar N, Kamdi DB. Thermal behavior of a finite hollow cylinder in context of fractional thermoelasticity with convection boundary conditions. J Therm Stress 2020;43:1189−1204. [CrossRef]
[25] Verma J, Lamba NK, Deshmukh KC. Memory impact of hygrothermal effect in a hollow cylinder by theory of uncoupled-coupled heat and moisture. Multidiscip Model Mater Struct 2022;18:826−844. [CrossRef]
[26] Youssef HM. Theory of fractional order generalized thermoelasticity. J Heat Transf 2010;132:1−7. [CrossRef]
[27] Abouelregal AE. The effect of temperature-dependent physical properties and fractional thermoelasticity on non-local nanobeams. J Math Theor Phys 2018;1:49−58. [CrossRef]
[28] Rashad AM, Chamkha AJ, Mallikarjuna B, Abdou MMM. Mixed bioconvection flow of a nanofluid containing gyrotactic microorganisms past a vertical slender cylinder. Front Heat Mass Transf 2018;10:10−21. [CrossRef]
[29] Rashad AM, Khan WA, EL-Kabeir SMM, EL-Hakiem AMA. Mixed convective flow of micropolar nanofluid across a horizontal cylinder in saturated porous medium. Appl Sci 2019;9:5241. [CrossRef]
[30] Rashad AM, Abbasbandy S, Chamkha AJ. Non-Darcy natural convection from a vertical cylinder embedded in a thermally stratified and nano-fluid-saturated porous media. J Heat Transf 2014;136:HT-13-1078. [CrossRef]
[31] Murali G, Paul A, Babu NN. Numerical study of chemical reaction effects on unsteady MHD fluid flow past an infinite vertical plate embedded in a porous medium with variable suction. Electron J Math Anal Appl 2015;3:179−192. [CrossRef]
[32] Deepa G, Murali G. Effects of viscous dissipation on unsteady MHD free convective flow with thermophoresis past a radiate inclined permeable plate. Iran J Sci 2014;38:379−388.
[33] El-Sayed AMA, Gaber M. On the finite Caputo and finite Riesz derivatives. Electron J Theor Phys 2006;3:81−95.
[34] Fil'Shtinskii LA, Kirichok TA, Kushnir DV. One-dimensional fractional quasi-static thermoelasticity problem for a half-space. WSEAS Trans Heat Mass Transf 2013;2:31−36.
[35] Ciesielski M, Leszczynski J. Numerical solutions to boundary value problem for anomalous diffusion equation with Riesz-Feller fractional operator. J Theor Appl Mech 2006;44:393−403.
[36] Momani Sh. General solutions for the space and time-fractional diffusion-wave equation. J Phys Sci 2006;10:30−43.
[37] Povstenko Y. Theories of thermal stresses based on space−time-fractional telegraph equations. Comput Math Appl 2012;64:3321−3328. [CrossRef]
[38] Assiri TA. Time-space variable-order fractional nonlinear system of thermoelasticity: numerical treatment. Adv Differ Equ 2020;288. [CrossRef]
[39] Ozdemir N, Avci D, Iskender DB. The numerical solutions of a two-dimensional space-time Riesz-Caputo fractional diffusion equation. Int J Optim Control 2011;1:17−26. [CrossRef]
[40] Atta D. Thermal diffusion responses in an infinite medium with a spherical cavity using the Atangana-Baleanu fractional operator. J Appl Comput Mech 2022;8:1358−1369.
[41] Abouelregal AE, Moustapha MV, Nofal TA, Rashid S, Ahmad H. Generalized thermoelasticity based on higher-order memory-dependent derivative with time delay. Results Phys 2021;20:103705. [CrossRef]
[42] Abouelregal AE, Sedighi HM, Faghidian SA, Shirazi AH. Temperature-dependent physical characteristics of the rotating nonlocal nanobeams subject to a varying heat source and a dynamic load. Facta Univ 2021;19:633−656. [CrossRef]
[43] Abouelregal AE, Atta D, Sedighi HM. Vibrational behavior of thermoelastic rotating nanobeams with variable thermal properties based on memory-dependent derivative of heat conduction model. Arch Appl Mech 2023;93:197−220. [CrossRef]
[44] Abouelregal AE, Askar SS, Marin M, Badahiould M. The theory of thermoelasticity with a memory-dependent dynamic response for a thermo-piezoelectric functionally graded rotating rod. Sci Rep 2023;13:9052. [CrossRef]
[45] Lamba NK, Verma J, Deshmukh KC. A brief note on space-time fractional order thermoelastic response in a layer. Appl Appl Math Int J 2023;18:1−9.
[46] Ozisik MN. Boundary value problems of heat conductions. Pennsylvania: Scranton; 1986.